

# A Chain-Driven, Sandwich-Legged Quadruped Robot: Design and Experimental Analysis

Aman Singh<sup>1</sup>, Bhavya Giri Goswami<sup>2</sup>, Ketan Nehete<sup>3</sup>, and Shishir N. Y. Kolathaya<sup>4</sup>

**Abstract**—This paper introduces a chain-driven, sandwich-legged, mid-size quadruped robot designed as an accessible research platform. The design prioritizes enhanced locomotion capabilities, improved reliability and safety of the actuation system, and simplified, cost-effective manufacturing processes. Locomotion performance is optimized through a sandwiched leg design and a dual-motor configuration, reducing leg inertia for agile movements. Reliability and safety are achieved by integrating robust cable strain reliefs, efficient heat sinks for motor thermal management, and mechanical limits to restrict leg motion. Simplified design considerations include a quasi-direct drive (QDD) actuator and the adoption of low-cost fabrication techniques, such as laser cutting and 3D printing, to minimize cost and ensure rapid prototyping. The robot weighs approximately 25 kg and is developed at a cost under \$8000, making it a scalable and affordable solution for robotics research. Experimental validations demonstrate the platform’s capability to execute trot and crawl gaits on flat terrain and slopes, highlighting its potential as a versatile and reliable quadruped research platform.

**Keywords:** Legged Robot, Quadruped Robot, Actuator, QDD Actuator, Robotic Leg, Design

## I. INTRODUCTION

Legged robots hold immense potential to revolutionize the way robots are deployed in diverse real-world scenarios. Their ability to lift and maneuver their legs during locomotion enables them to navigate unstructured terrains. This capability makes legged robots invaluable for applications such as power-plant inspections in hazardous factory environments, transporting goods in hilly or uneven terrains, and serving as first responders in disaster-stricken areas.

However, developing reliable legged robotic systems demands not only robust and adaptive control algorithms but also rigorous testing on physical hardware. Such testing is essential to bridge the gap between theoretical models and practical deployments. The progress in this domain critically depends on accessible, functional, and dependable robot platforms that serve as testbeds for researchers. While various quadruped robotic systems exist globally for algorithm testing, further advancements in hardware design and accessibility are crucial to accelerate innovation in this field.

\*This work is supported by the SERB core research grant: CRG/2021/008115, and Pratiksha Trust Young Investigator Fellowship.

<sup>1</sup>Aman Singh and Shishir N. Y. Kolathaya are with the Robert Bosch Center for Cyber Physical Systems, Indian Institute of Science, Bengaluru.

<sup>2</sup>Bhavya Giri Goswami is with University of Waterloo, Waterloo, Ontario, Canada

<sup>3</sup>Ketan Nehete is with UC Berkeley, Berkeley, California, United States

<sup>4</sup>S. Kolathaya is with the Robert Bosch Center for Cyber Physical Systems and the Department of Computer Science & Automation, Indian Institute of Science, Bengaluru. (email: stochlab@iisc.ac.in)



Fig. 1. Chain-driven, Sandwich-legged quadruped robot shown standing on the ground.

The MIT Cheetah-3[1] exemplifies a highly versatile quadruped capable of dynamic motions, such as jumping onto elevated surfaces, owing to its high-torque-density custom motors. However, these motors require advanced manufacturing techniques, leading to high development costs. Similarly, the MIT Mini-Cheetah[2] features a lightweight design, enabled by modular actuators with planetary gearboxes integrated inside the stator core of the outrunner BLDC motors. This design supports dynamic movements, including backflips, but demands complex processes such as machining the motor’s stator or using frameless motors.

Stanford Doggo [3] is an open-source, lightweight quadruped with torque-controlled joints, making it cost-effective for research. However, its 2-DOF legs limit its ability to test advanced locomotion. Similarly, Mini-Taur [4] uses direct-drive principles for transparency and high-bandwidth control but suffers from joule heating due to its gearbox-free design and limited 2-DOF leg functionality.

In contrast, the KAIST Hound[5] incorporates a parallel actuator configuration for hip and knee joints, requiring precision manufacturing to address the mechanical complexity of its design, thus increasing costs. Panther[6][7], another research platform, features a simple design methodology with compound planetary gearbox actuators. However, the

separation of motor drivers from actuators adds wiring complexity, potentially affecting reliability.

Hydraulically actuated systems, such as the HyQ robot[8], provide high power and force density, making them ideal for high-load applications. Yet, their heavy, inefficient, and complex designs pose significant drawbacks. Similarly, the ANYmal[9] robot, employing harmonic drives and series elastic actuators, ensures precise torque control and impact resistance but sacrifices control bandwidth and simplicity, increasing manufacturing costs.

Open-source robots like Solo[10] adopt simplified designs using 3D-printed and off-the-shelf components, making them accessible for research. However, its timing belt transmission is prone to slippage under high loads, reducing reliability. Barry[11], designed for high payloads, relies on ball-screw linkages and frameless BLDC motors, introducing complexity and compromising simplicity.

Finally, commercial platforms like Spot[12], Vision60[13], and Go1[14] offer reliability but lack publicly available design details. Additionally, Spot and Vision60 are prohibitively expensive, limiting their adoption for research purposes.

From the analysis, numerous quadrupedal platforms showcase excellent locomotion but often face trade-offs. Systems like [1], [2], [5], [11], and [9] rely on complex designs requiring precision-manufactured components, increasing costs. Simpler designs, such as [3] and [4], are limited by 2-DOF legs, while others, like [10], and [7], [6], face potential reliability concerns. Commercial robots are either expensive or lack open designs, restricting their utility in research.

In this paper, we present a quasi-direct drive quadrupedal research platform with a chain-sprocket system to drive the knees. We describe its hardware development, design choices to enhance locomotion capability and reliability of the actuator system, and design principles ensuring low cost and rapid manufacturing.

The main contributions of the paper are as follows.

- A chain-driven quasi-direct drive (QDD) actuator with an integrated planetary gearbox and motor driver. This eliminates the need for machining off-the-shelf motors or using frameless motors[2], [11], [5].
- A sandwiched leg design aimed at reducing leg inertia and manufacturing costs. It features a lightweight composite core sandwiched between two laser-cut metal sheets, providing both strength and reduced weight. This approach offers an alternative to CNC-intensive methods used in [1], [7], [9], [2], [8], [5], [11].
- A torso design, using sheet metal and plastic. It reduces cost and fabrication time while maintaining strength.

The paper is organized as follows: Section II will describe the robot's design and also explain the design principles. Section III will describe the electronics and control architecture. Section IV will provide results on hardware walking, and qualitative measures of the reliability steps taken. Finally, Section V will provide conclusions and discuss future work.

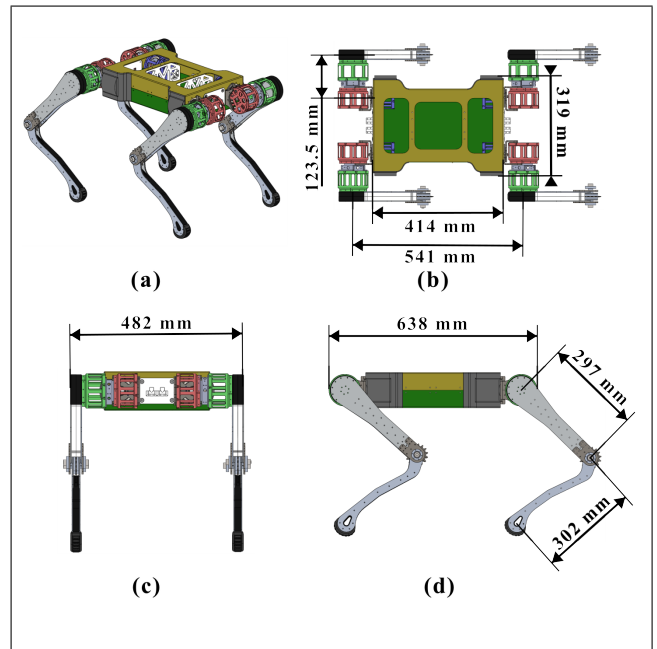


Fig. 2. **Robot Dimensions:** (a) Isometric view of the robot: The torso is made up of two sheet metal parts (yellow and green), with two plastic parts (white and inside the torso) joining them (b) Top view, (c) Front View, (d) Side view

## II. DESIGN

This section explains the design of the custom-built dynamic quadruped robot, shown in Fig.1. Each leg has 3 actuated degrees of freedom, controlled by a modular Quasi-Direct-Drive (QDD) actuator with single staged planetary gearbox. The robot does not contain any foot contact sensor or foot force sensor, and detects ground contact using joint actuator currents. The dimensions of the robot are given in the Fig.2. The robot weighs approximately 25 Kg.

While designing the robot we took several design decisions to enhance the locomotion capability of the robot, make its actuation system more reliable and safe, and make the design simpler to reduce the cost and complexity of manufacturing. We will discuss those decisions in detail.

### A. Simplified Design

1) *QDD Actuator:* The robot utilizes a custom-built quasi-direct-drive actuator, featuring an off-the-shelf BLDC motor (T-motor, U10 plus, Kv100) paired with a 6:1 single-stage planetary gear reduction and a moteus r4.10 motor driver from MJBOTS [15] (Fig. 3). The actuator incorporates KHK gears with a 0.8 mm module, where the sun gear has 20 teeth, the planet gear has 40 teeth, and the ring gear has 100 teeth. Post-purchase machining was performed to customize the gears. Weighing approximately 920 g, the actuator's motor driver includes an onboard Hall effect sensor, allowing it to be mounted directly on the actuator module for a compact design and reduced wiring.

2) *Design for efficient manufacturing:* To minimize manufacturing cost and time, the robot's components were designed to enable efficient fabrication processes without com-

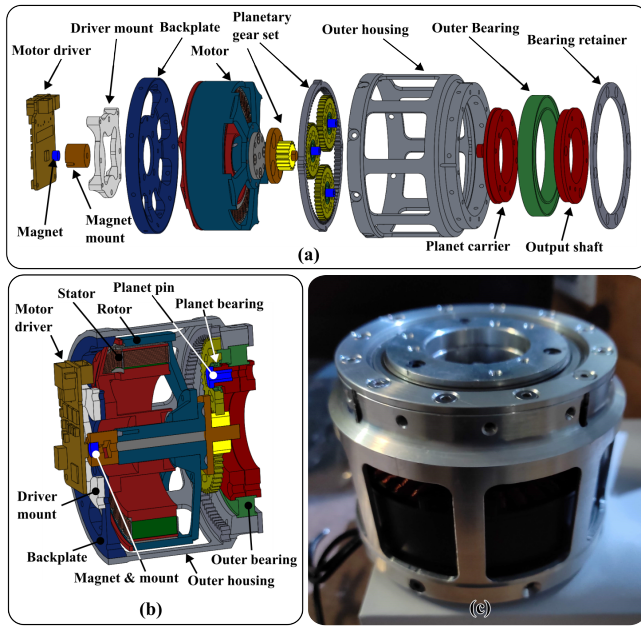


Fig. 3. **QDD Actuator:** (a) Details of the actuator design; (b) Cross-section view of actuator; (c) Manufactured actuator

promising structural integrity. The design extensively utilizes metal laser cutting and 3D printing for fast production.

The torso consists of a cuboid-shaped box made from two sheet metal parts, which are laser cut and bent (Fig. 4). These two sheet metal parts are connected by two 3D-printed rectangular components, and the abduction actuators are mounted at each corner to provide additional strength. This design reduces fabrication time and cost while maintaining structural strength. The 3D-printed parts inside the torso also serve as mounting points for the electronics.

As will be discussed in the sandwiched leg design section, the robot’s legs are constructed from laser-cut sheet metal, and 3D-printed plastic components (Fig. 5). The metal parts provide strength, while the plastic components act as spacers and shape-defining elements. The abduction-to-hip coupling, which is crucial for bearing forces during walking, is also fabricated using laser-cut and bent sheet metal for strength and fast production. Additionally, the tensioner for the knee joint chain is made from laser-cut steel parts.

### B. Enhancement of Locomotion Capability

To enhance locomotion capabilities, low leg inertia is crucial as it facilitates faster leg movements and reduces actuator effort during walking. We propose two design criteria: a sandwich leg design and a dual motor architecture, which effectively achieve low leg inertia. These approaches are discussed in detail below.

1) *Sandwiched Leg Design:* The robot’s leg consists of three links: the abduction link, the thigh link, and the shank link, as shown in Fig. 5(b). The abduction link includes the abduction/adduction (Ab/Ad)-to-hip-coupling and the outer shell of the hip actuator. The thigh and shank links are

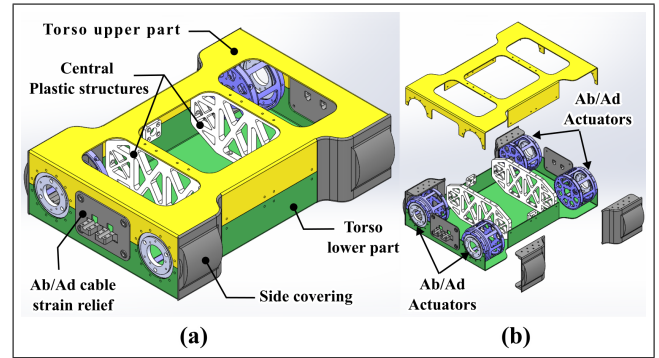


Fig. 4. **Torso Diagram:** (a) Details of Torso design (b) Exploded view of Torso

designed using a “sandwich” structure of sheet metal and plastic.

The sandwich leg design incorporates two sheet metal plates with a 3D-printed plastic component positioned between them, as illustrated in Fig. 5(c,d). The metal plates provide structural strength, while the plastic part contributes to the form and shape of the legs and serves as a spacer. These components are securely joined using superglue and fasteners.

To address the high loads experienced at the knee joint during locomotion, the regions near the knee joint in the thigh and shank links are reinforced with steel plates, as shown in Fig. 5(c,d). This lightweight design reduces leg inertia, enhancing locomotion performance, and aligns with the simplified design philosophy discussed earlier.

2) *Dual Motor Design:* The dual motor architecture [16] draws inspiration from animals like horses, utilizing large proximal muscles and lightweight distal limbs to reduce leg inertia and enhance locomotion efficiency. In this robot’s design, both hip and knee actuators are positioned near the hip joint, eliminating the need for a knee-mounted actuator, thereby significantly reducing leg inertia.

The knee joint is powered through a chain mechanism, although a timing-belt mechanism could be implemented with minor modifications. Here, the rotor of the hip actuator is coupled to the stator (outer body) of the knee actuator, which is mounted on the thigh link. The knee actuator drives a sprocket that transmits power to the knee joint via the chain mechanism.

This mechanism not only transmits power but also allows for extra gear reduction at the knee joint by varying sprocket sizes. The driving sprocket has 11 teeth and the driven sprocket has 15 teeth, resulting in an effective gear reduction of 8.18:1 (both planetary and chain), crucial for enhancing the knee joint’s torque capacity during locomotion.

### C. Reliability and safety of actuation system

The robot was designed as a research platform capable of operating in both indoor and outdoor environments. When navigating rough outdoor terrains, the platform experiences erratic motion, which can lead to disconnections of the actuator wires that move with the articulated limbs. Additionally,



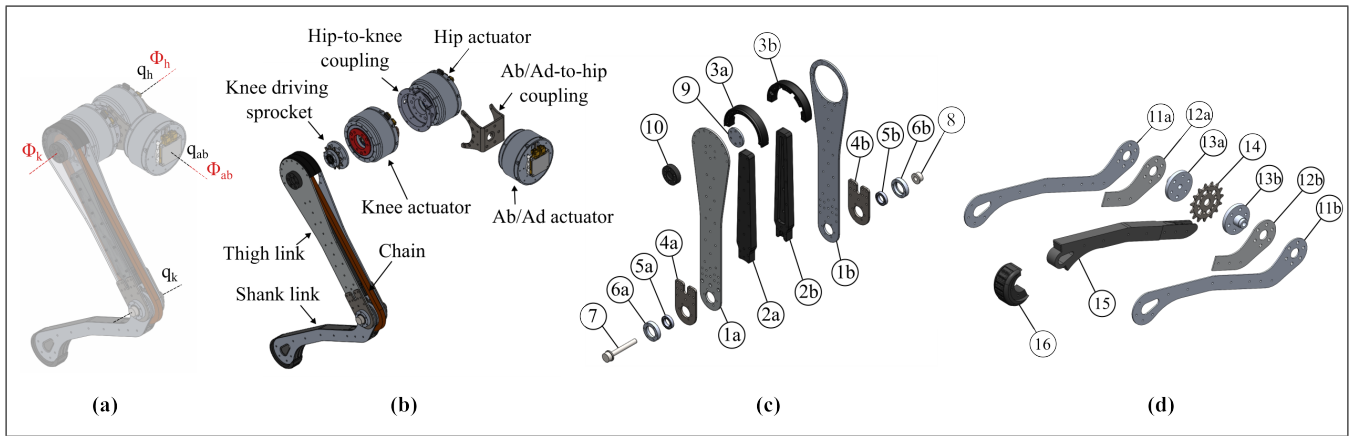


Fig. 5. (a) Joints and Actuator Axes; (b) Details of Leg Design; (c) Details of Thigh Link: ①a, ①b: Al Sheets; ②a, ②b: Central spacers; ③a, ③b: Upper spacers; ④a, ④b: Thigh strength plates; ⑤a, ⑤b: Knee bearings; ⑥a, ⑥b: Knee bearing blocks; ⑦: Knee bolt; ⑧: Knee nut; ⑨: Sprocket support shaft; ⑩: Support shaft fastener; (d) Details of Shank Link: ①a, ①b: Shank Al-sheets; ②a, ②b: Shank strength plates; ③a, ③b: Knee sprocket couplings; ④: Knee driven sprocket; ⑤: Shank spacer; ⑥: Foot.

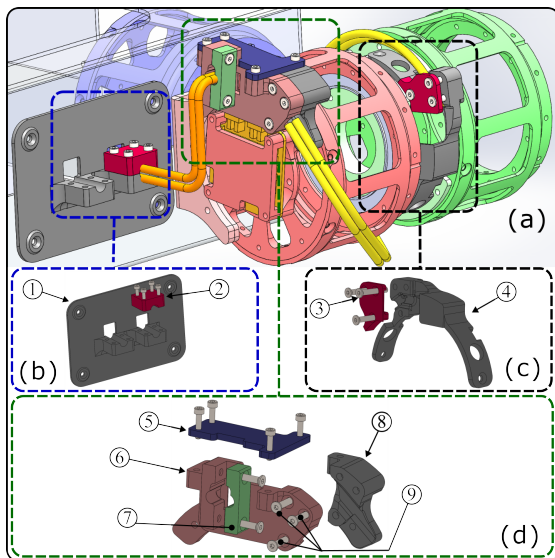


Fig. 6. **Cable Strain Reliefs:** (a) Anatomy of cables and strain reliefs; (b) Ab/Ad strain relief: ① is mounted on the torso, ② fastens the wire coming from the Ab-Ad actuator (orange wire); (c) Knee strain relief: ④ is mounted on the hip-to-knee coupling, and ③ fastens the wire coming from the Hip actuator (yellow wire); (d) Hip strain relief: ⑧ and ⑨ is mounted on the hip actuator, ⑥ and fasteners ⑦ are used to fasten the wire going to the Knee actuator (yellow wire), ⑦ secures the wire coming from the Ab-Ad actuator (orange wire), and ⑤ helps push the wires from the top.

long-distance locomotion in outdoor conditions can cause motor drivers to overheat significantly, potentially degrading performance or causing complete failure. As the robot will also be tested with various new control algorithms, some of which may be erroneous, there is a risk to researchers working near the robot.

To mitigate these challenges, enhancing the reliability and safety of the actuation systems is crucial. To address this, three key measures were implemented to improve the system's robustness and safety.

1) *Cable Strain Relief:* Cable strain reliefs are designed to securely fix the actuator connection wires, preventing

disconnections during locomotion. The wiring is arranged in a daisy-chain configuration in each leg, meaning that instead of running separate wires to each actuator, the wires from the main electronics are routed through the abduction actuator, then the hip actuator, and finally to the knee actuator, forming a series connection.

The strain relief for the abduction actuator is attached directly to the torso. The wires from the main electronics first connect to the abduction actuator, and then they pass through a hole in the abduction cable strain relief, which is rigidly fastened to the torso using fasteners, as shown in Fig. 6(a, b). For the hip actuator, the cable strain relief secures two connections: one from the abduction actuator and another leading to the knee actuator. The design details are shown in Fig. 6(a, d). The knee actuator's cable strain relief fixes only one connection. The knee motor driver is housed within the cavity of the hip-to-knee coupling (Fig. 7(a)). The wires are routed through a hole in the coupling, and the knee strain relief is mounted over this hole to securely attach the wire from the hip actuator. The design details are shown in Fig. 6(a, c).

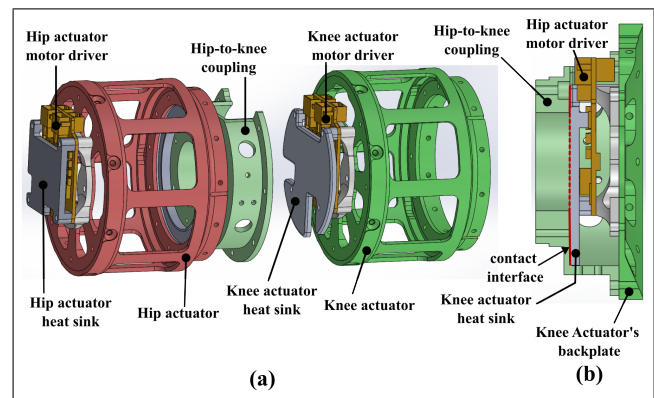


Fig. 7. **Thermal Management:** (a) Exploded view: The knee heat sink goes inside the cavity of the Hip-to-knee coupling; (b) Cross-section view: The knee heat sink touches the Hip-to-knee coupling at the contact interface (red).



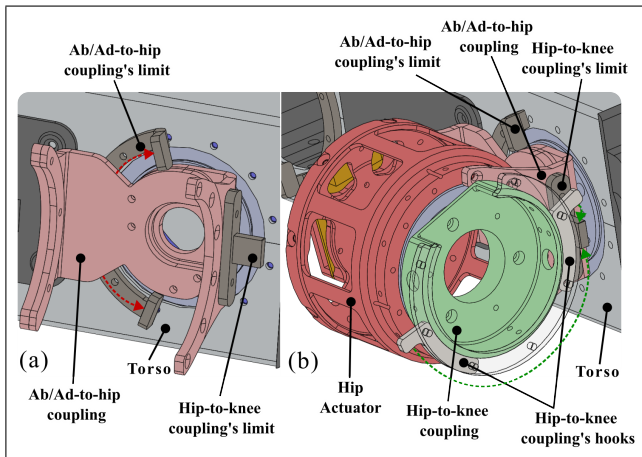


Fig. 8. **Safety Limits:** (a) Ab/Ad-to-hip coupling limit; (b) Hip-to-knee coupling limit

2) *Thermal Management:* Off-the-shelf heat sinks were used for the abduction and hip actuators, sourced from [15]. For the knee actuators, custom-designed heat sinks were fabricated due to the significant heating of the knee actuator's motor drivers, which resulted in reduced operational uptime for the robot. The knee actuator's heat sink, as shown in Fig. 7, makes contact with the MOSFETs and driver board on one side, and with the hip-to-knee coupling on the other. The coupling, in turn, is in contact with the knee actuator's outer shell, thereby increasing the overall thermal capacity. Thermal paste was applied between the MOSFETs and the heat sink, as well as between the heat sink and the hip-to-knee coupling, to enhance thermal conductivity. Additionally, the heat sink serves a dual purpose by protecting the previously exposed motor driver of the hip actuator from potential physical damage.

3) *Safety Limits:* Mechanical safety limits are incorporated into each leg joint to restrict the range of motion, ensuring operator safety while testing the robot platform. The Ab/Ad joint is limited by the Ab/Ad-to-hip coupling's limit, while the hip joint is restricted by the hip-to-knee coupling's limit, as shown in Fig. 8.

The Ab/Ad joint limit is fixed to the torso, while the hip joint limit is attached to the Ab/Ad-to-hip coupling. Hooks on the hip-to-knee coupling contact the hip joint limit to restrict motion. Both limits and hooks are fabricated from laser-cut and bent steel sheets, while the knee joint is constrained by the thigh link, eliminating the need for separate mechanical limits.

The allowable joint ranges of motion are  $\pm 35^\circ$  for the Ab-Ad joint,  $+75^\circ$  to  $-60^\circ$  for the hip joint, and  $+165^\circ$  to  $-55^\circ$  for the knee joint. These ranges can be extended with minor modifications to the design of the limits and hooks, providing flexibility for future improvements.

### III. ELECTRONICS AND CONTROL ARCHITECTURE

The locomotion control of the robot is executed on a Raspberry Pi 4B (RPI) microcomputer paired with an mjbots

pi3hat board, which facilitates low-level communication between the RPI and the motor drivers on each leg. Communication with the three actuators per leg is achieved using four independent CAN buses. Each actuator is equipped with an mjbots moteus r4.10 motor driver featuring onboard Hall-effect encoders for angle and velocity measurement via the CAN bus. For orientation and motion sensing, the robot utilizes an Xsens MTi-610 Inertial Measurement Unit (IMU), providing calibrated 3D orientation, angular velocities, and accelerations.

The robot is powered by a 22.2 V, 10,000 mAh Li-Po battery pack housed in a sliding box with a simple nut-bolt interface for convenient battery swapping. Power distribution is managed by two off-the-shelf mjbots power distribution boards, with power routed efficiently to the leg actuators using a daisy-chain configuration. Additionally, the robot's torso has ample space to accommodate an extra onboard computer for high-level computation, such as image processing or other advanced tasks.

The control architecture is inspired by [17] and incorporates a linear policy coupled with a lower-level controller. The linear policy generates trajectory modifications and body-wrench values, which the lower-level controller transforms into joint torque commands [18]. This setup was designed to evaluate the actuator's torque control capabilities.

## IV. RESULTS

This section presents the results of the design decisions taken and discussed in the Design section, hardware walking results and also some potential improvements on the design which we got after extensive testing of the robot.

### A. Design Principles Results

This subsection highlights the effects of key design decisions on the reliability and performance of the robot.

1) *Simplified Design:* The simplified design principles utilized sheet metal cutting and bending, combined with 3D-printed components, to construct the robot's torso and legs. Using off-the-shelf motors, gears, and drivers kept costs below \$8000, with approximately \$4500 for motors and \$3500 for electronics and manufactured parts, making it a cost-effective midsized robot platform.

2) *Enhancement of Locomotion Capability:* The sandwiched leg design and dual-motor architecture reduced leg inertia, enhancing locomotion capability. Each leg's lightweight design (1.5 Kg/leg) enabled faster control responses and effective movement across diverse terrains.

3) *Reliability and Safety of the Actuation System:* Key design improvements enhanced the actuator system's reliability and safety. Cable strain reliefs effectively resolved disconnection issues observed in early prototypes during locomotion. Thermal management, achieved by connecting the knee actuator heat sink to the hip-to-knee coupling with thermal paste, increased operating time from 10 to 30 minutes. Mechanical joint limits ensured both operator's safety and robot's protection from self-damage during operation.

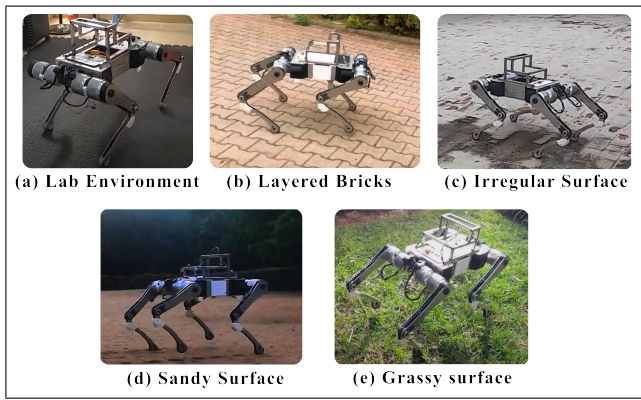


Fig. 9. Robot walking on different surfaces

### B. Hardware Experiment Results

The hardware platform was tested in real-world scenarios to validate its effectiveness. Experiments included testing in laboratory environments, navigating uneven outdoor terrains such as sand and grass with a trot gait, and handling external disturbances (Fig. 9).

## V. CONCLUSION AND FUTURE WORK

This paper presented the design and development of a chain-driven, sandwich-legged quadruped robot, emphasizing simplified design principles, enhanced locomotion capabilities, and reliable actuation. The use of QDD actuators, sheet metal fabrication, and 3D printing enabled cost-effective manufacturing without compromising strength. Key features, such as the dual-motor architecture and sandwiched leg design, improved locomotion, while reliability was ensured through cable strain reliefs, thermal management, and safety limits. Hardware experiments validated the robot's ability to traverse outdoor uneven terrains and reject external disturbances.

Testing feedback highlighted several areas for improvement, which will guide future work. The current torso design, comprising two sheet metal components with abduction actuators mounted on both parts, experiences bending due to high forces at the mounting locations. To address this, a thicker metal plate will be used to enhance structural integrity. The knee actuator, which bears significant loads, causes motor driver overheating. Improved thermal management will be achieved by integrating the knee heat sink with the hip-to-knee coupling into a single component and adding fins to increase the surface area for better cooling. Additionally, the current foot, made from silicone molding, wears quickly on abrasive terrains despite sustaining required loads. Future iterations will employ vulcanized rubber to enhance durability and longevity in outdoor environments.

## REFERENCES

[1] G. Bledt, M. J. Powell, B. Katz, J. Di Carlo, P. M. Wensing, and S. Kim, "Mit cheetah 3: Design and control of a robust, dynamic quadruped robot," in *2018 IEEE/RSJ International Conference on Intelligent Robots and Systems (IROS)*, 2018, pp. 2245–2252.

[2] B. Katz, J. D. Carlo, and S. Kim, "Mini cheetah: A platform for pushing the limits of dynamic quadruped control," in *2019 International Conference on Robotics and Automation (ICRA)*, 2019, pp. 6295–6301.

[3] N. Kau, A. Schultz, N. Ferrante, and P. Slade, "Stanford doggo: An open-source, quasi-direct-drive quadruped," 05 2019, pp. 6309–6315.

[4] G. Kenneally, A. De, and D. E. Koditschek, "Design principles for a family of direct-drive legged robots," *IEEE Robotics and Automation Letters*, vol. 1, no. 2, pp. 900–907, 2016.

[5] Y.-H. Shin, S. Hong, S. Woo, J. Choe, H. Son, G. Kim, J.-H. Kim, K. Lee, J. Hwangbo, and H.-W. Park, "Design of kaist hound, a quadruped robot platform for fast and efficient locomotion with mixed-integer nonlinear optimization of a gear train," in *2022 International Conference on Robotics and Automation (ICRA)*, 2022, pp. 6614–6620.

[6] Y. Ding, A. Pandala, C. Li, Y.-H. Shin, and H.-W. Park, "Representation-free model predictive control for dynamic motions in quadrupeds," *IEEE Transactions on Robotics*, vol. 37, no. 4, pp. 1154–1171, 2021.

[7] Y. Ding and H.-W. Park, "Design and experimental implementation of a quasi-direct-drive leg for optimized jumping," in *2017 IEEE/RSJ International Conference on Intelligent Robots and Systems (IROS)*, 2017, pp. 300–305.

[8] C. Semini, N. G. Tsagarakis, E. Guglielmino, M. Focchi, F. Cannella, and D. G. Caldwell, "Design of hyq - a hydraulically and electrically actuated quadruped robot," *IMEchE Part I: Journal of Systems and Control Engineering*, vol. 225, no. 6, pp. 831–849, 2011.

[9] M. Hutter, C. Gehring, D. Jud, A. Lauber, C. D. Bellicoso, V. Tsounis, J. Hwangbo, K. Bodie, P. Fankhauser, M. Bloesch, R. Diethelm, S. Bachmann, A. Melzer, and M. Hoepflinger, "Anymal - a highly mobile and dynamic quadrupedal robot," in *2016 IEEE/RSJ International Conference on Intelligent Robots and Systems (IROS)*, 2016, pp. 38–44.

[10] F. Grimmering, A. Meduri, M. Khadiv, J. Viereck, M. Wüthrich, M. Naveau, V. Berenz, S. Heim, F. Widmaier, T. Flayols, J. Fiene, A. Badri-Spröwitz, and L. Righetti, "An open torque-controlled modular robot architecture for legged locomotion research," *IEEE Robotics and Automation Letters*, vol. 5, no. 2, pp. 3650–3657, 2020.

[11] G. Valsecchi, N. Rudin, L. Nachtigall, K. Mayer, F. Tischhauser, and M. Hutter, "Barry: A high-payload and agile quadruped robot," *IEEE Robotics and Automation Letters*, vol. 8, no. 11, pp. 6939–6946, 2023.

[12] B. Dynamics, "Spot® - the agile mobile robot," <https://bostondynamics.com/products/spot/>, 2024, accessed: Dec 5, 2024.

[13] G. Robotics, "Vision 60," <https://www.ghostrobotics.io/vision-60>, 2024, accessed: Dec 5, 2024.

[14] Unitree, "Unitree go-1," <https://shop.unitree.com>, 2024, accessed: Dec 5, 2024.

[15] MJBOTS, "Mjbots," <https://mjbots.com/>, 2024, accessed: Dec 5, 2024.

[16] S. Seok, A. Wang, M. Y. Chuah, D. Otten, J. Lang, and S. Kim, "Design principles for highly efficient quadrupeds and implementation on the mit cheetah robot," in *2013 IEEE International Conference on Robotics and Automation*, 2013, pp. 3307–3312.

[17] M. Rahme, I. Abraham, M. L. Elwin, and T. D. Murphey, "Linear policies are sufficient to enable low-cost quadrupedal robots to traverse rough terrain," in *2021 IEEE/RSJ International Conference on Intelligent Robots and Systems (IROS)*, 2021, pp. 8469–8476.

[18] A. Shirwatkar, V. K. Kurva, D. Vinoda, A. Singh, A. Sagi, H. Lodha, B. G. Goswami, S. Sood, K. Nehete, and S. Kolathaya, "Force control for robust quadruped locomotion: A linear policy approach," in *2023 IEEE International Conference on Robotics and Automation (ICRA)*, 2023, pp. 5113–5119.